SAND99-2031C

Modeling Transport in Gas Chromatography Columns for the Micro-ChemLab™

C. Channy Wong, Douglas R. Adkins, Gregory C. Frye-Mason, Mary L. Hudson, Richard Kottenstette, Carolyn M. Matzke, John N. Shadid, and Andrew G. Salinger

Sandia National Laboratories
Albuquerque, New Mexico 87185

ABSTRACT

The gas chromatography (GC) column is a critical component in the microsystem for chemical detection (μChemLab™) being developed at Sandia. The goal is to etch a 'meter-long' GC column onto a 1-cm^2 silicon chip while maintaining good chromatographic performance. Our design strategy is to use a modeling and simulation approach. We have developed an analytical tool that models the transport and surface interaction process to achieve an optimized design of the GC column. This analytical tool has a flow module and a separation module. The flow module considers both the compressibility and slip flow effects that may significantly influence the gas transport in a long and narrow column. The separation module models analyte transport and physico-chemical interaction with the coated surface in the GC column. It predicts the column efficiency and performance. Results of our analysis will be presented in this paper.

In addition to the analytical tool, we have also developed a time-dependent adsorption/desorption model and incorporated this model into a computational fluid dynamics (CFD) code to simulate analyte transport and separation process in GC columns. CFD simulations can capture the complex three-dimensional flow and transport dynamics, whereas the analytical tool cannot. Different column geometries have been studied, and results will be presented in this paper. Overall we have demonstrated that the modeling and simulation approach can guide the design of the GC column and will reduce the number of iterations in the device development.

KEY WORDS: Micro-ChemLab, Gas chromatography, Adsorption/desorption, Separation, Microscale transport

NOMENCLATURE

D_g	Diffusion coefficient of analyte in carrier gas
D_s	Diffusion coefficient of analyte in stationary layer
d	Column width
F	Effective to actual surface area of stationary layer
H	Column height
h	Theoretical plate height
Kn_o	Knudsen number at outlet
k	Retention factor
L	Column length
P_i	Inlet pressure
P_o	Outlet pressure
R	Radius of curvature
u_o	Gas velocity at outlet
w	Thickness of stationary layer
Δc	Change in molar concentration
Δt	Sum of instrumental dead times
$\Delta\tau$	Time delay from adsorption to desorption
ρ	Density of carrier gas
μ	Viscosity of carrier gas

*Correspondence: Email: ccwong@sandia.gov; Telephone: 505 844 3530; Fax: 505 844 4523

DISCLAIMER

1. INTRODUCTION

At present Sandia National Laboratories is developing an integrated microsystem for detecting chemicals at the trace level (μChemLab™). This μChemLab™ will be a small hand-held device. It will contain both the liquid[1] and gas phase[2] detection units. For the gas phase detection unit, the major components are:

- Preconcentrator (PC) for analyte (or sample) collection,
- Gas chromatography (GC) column for separation,
- Surface acoustic wave (SAW) array mass detector for sensing,
- Pump and valve for fluid control.

Figure 1 shows three of these major components. They have been designed and fabricated at Sandia. At present the first generation of the μChemLab™ will use a commercial diaphragm pump and a miniature valve. This paper will be focused on the development of the GC column.

For a better performance of chemical detection, it is always important to have well-separated analytes in the GC column. Hence designing an efficient column is crucial to the success of the micro-chemical detection system. Conventional GC columns are silica tubes of about 250 microns in diameter and about 20 m long[3]. These columns have a thin liquid layer coated onto the walls, typically, 10 nm thick. The variation in adsorption equilibrium will cause different analytes to interact differently with the surface coating material. This difference in reaction kinetics will lead to different migrating speeds of analytes through the GC column. The variation in migration speed is one mode of separation in gas chromatography[4].

1.1. Gas Chromatography on a Chip

For the μChemLab™ project at Sandia, our goal is to reduce the dimensions of the GC column so that it can fit onto a 1-cm^2 silicon chip while achieving good separation efficiency and short run time (Fig. 1). Can a micro GC column work better than a conventional GC column? This is an important question that needs to be addressed. We have reviewed existing models to study the transport and separation process in GC columns. Our study indicates that the performance of chromatography depends on the ratio of length-to-width of the column. As the size of the column decreases, one can achieve a similar performance (same number of theoretical plates) with a shorter column. This study further leads us to develop an analytical model for design and optimization.

The GC columns on a silicon wafer (GC on a chip) are fabricated at Sandia using the Bosch deep reaction ion etch (RIE) process[5]. This process uses an alternating sequence of plasma etching and polymer deposition to keep the side walls of the column vertical, while the bottom wall continues to be etched. After the etch and removal of the photoresist, the etched column area is anodically sealed with a Pyrex cover slip. Hence at the end of the process, these GC columns have the following unique characteristics:

1. The column will be a 'high-aspect-ratio' rectangular channel (Fig. 2). This design is to achieve the desired volumetric flow rate and also to maximize the surface area-to-volume ratio.
2. The column is 1-meter long to obtain an efficient separation. Our model indicates that the length-to-width ratio needs to be about 20,000.
3. In order to fit the long column onto a small area, the column will have a tight spiral configuration.

To guide the design of this 'GC on a chip,' we have developed an analytical tool to predict the chromatographic performance of different GC columns. This analytical tool has a flow module and a separation module. In the next section description of these modules will be presented.

2. MODELING

2.1. Flow Studies

The flow module of the analytical tool models the gas transport in a GC column that has a long and narrow channel — e.g. a channel with an equivalent hydraulic diameter of 100 μm, total length of 1 m, and the length-to-diameter ratio of 10,000. Gas flow in this microchannel is a unique fluid dynamics problem. Even though the flow velocity is much smaller than the sound speed, the compressibility effect has to be considered. Since the channel is very small, the viscous effect becomes dominant, and the inertia effect becomes less important (but not negligible as in liquid flow where 'Stokes Flow'[6] can be applied). The pressure required to pump gas along the channel increases as the channel size decreases. For a long and narrow

channel, the pressure and density changes between inlet and outlet are enormous, which causes the flow to accelerate near the outlet. This leads to a higher mass flow rate than the prediction based on an incompressible flow. Hence when modeling this phenomenon, known as "compressible creep flow", we need to include the compressibility effect by incorporating a large change in pressure and density, even though gas is traveling at a very low subsonic speed.

As the column size decreases even further into the micron scale, the effect of slip flow at the boundary needs to be considered. From the kinetic theory of gases if the characteristic length of the physical domain (*d*) is small and compatible with the mean free path of the molecules (λ), the continuum hypothesis and no-slip boundary condition become invalid. At the standard atmospheric conditions, the mean free path of air is about 0.065 μm. The deviation of the state of the gas from continuum is measured by the Knudsen number (*Kn*), which is defined as $Kn=\lambda/d$. As the value of Knudsen number increases, rarefaction or noncontinuum effects become more important. A typical way to determine the continuum versus rarefied flow[7] is as follows:

For $Kn < 0.01$,	continuum flow regime
For $0.01 < Kn < 0.1$,	slip flow regime
For $0.1 < Kn < 10$,	transition regime
For $10 < Kn$,	free molecular flow regime

For the μChemLab™, gas flow in GC columns is generally in the continuum flow regime. However if the column size is reduced to below 10 μm, the gas flow will be in the slip flow regime. Hence the slip velocity at the boundary can be approximated as:

$$u_w = \left(\frac{2-\sigma_m}{\sigma_m}\right)\left(\lambda \left.\frac{\partial u}{\partial y}\right|_w\right) \tag{1}$$

where *y* is normal to the surface, and σ_m is the tangential momentum accommodation coefficient. For most surfaces σ_m lies between 0.8 and 1.0. For the μChemLab™ applications we assume σ_m equals one. In summary, for those cases where slip flow exists at the wall, the average flow velocity will be higher than the velocity in the no-slip case.

If considering both the gas compressibility and slip flow effects, the volumetric flow rate at the exit of the column can be found by solving the Navier-Stokes equations analytically. The following expression is obtained:

$$\dot{V}_o = (u_o \cdot d \cdot H) = \frac{d^3 H}{24}\frac{(P_i^2 - P_o^2 + 12Kn_o P_o(P_i - P_o))}{\mu L P_o}(1 - ARC) \tag{2}$$

where *ARC* is the aspect ratio correction with respect to the rectangular cross section. It can be found as follows:

$$ARC = \frac{192}{\pi^5}\cdot\frac{d}{H}\cdot\sum_{i=1,3,5}^{\infty}\frac{\tanh(i\pi H/2d)}{i^5} \tag{3}$$

Flow measurement in both capillary tubes and spiral GC columns have been performed, and their data has been used to assess the analytical model. Here the focus is to evaluate the exit volumetric flow rate as a function of the pressure drop across the channels. Predictions from the analytical model compare reasonably well with the measurement for the gas flow in the etched spiral columns (Fig. 3). The accuracy of the experimental data is about 1 percent for the flow rate and 1.5 percent for the pressure measurement. These columns are 40 μm wide with lengths of 0.3 and 1 m. The maximum Knudsen number for these cases is about 0.004, which indicates the flow is continuum. The difference in the flow rates calculated with slip and no-slip boundary condition is very small (less than 2 percent). However, slip flow does become important if the column size is reduced to 10 μm wide. In this situation the difference in volumetric flow rate, with and without slip, can be as high as 12 percent.

2.2. Separation Analysis

The second module involves modeling the analyte transport and physico-chemical interaction with the coated surface in the GC column to determine the performance of chromatography. As the analyte travels through the GC column, the analyte

band will be broadened and diluted. Hence the extent of this band spreading is an important measure of the GC performance. We have modified the Golay equation[8] to predict the band spreading for the rectangular cross-sectional column. The modified Golay equation is:

$$h = f_1\frac{B}{u_o} + f_1 C_g u_o + f_2 C_s u_o + (f_2 u_o)^2 E \qquad (4)$$

where h is expressed as the height of an equivalent theoretical plate or the HETP value[9]. This modified Golay equation is for an open column of uniform cross section and isothermal operation. It includes a pressure correction (f_1 and f_2) and an additional term for the instrumental contribution to band broadening (E). These four terms in the Golay equation represent the static and dynamic diffusion of the analyte in the carrier gas, diffusion of the analyte in the stationary layer, and the band broadening owing to the sum of the instrumental dead times, respectively[10]. The description of the coefficients in these terms can be found in Table 1.

Table 1: Analytical Expressions for the Coefficients in the Modified Golay Equation

B	C_g	C_s	E	f_1	f_2
$2D_g$	$\frac{4\left(1+9k+\frac{51}{2}k^2\right)\left(\frac{d}{2}\right)^2}{105(k+1)^2 D_g}$	$\frac{2kw^2}{3(k+1)^2 F^2 D_s}\left(\frac{H+d}{H}\right)^2$	$\frac{(\Delta t)^2}{L(k+1)^2}$	$\frac{9(P_i^4 - P_o^4)(P_i^2 - P_o^2)}{8(P_i^3 - P_o^3)^2}$	$\frac{3P_o(P_i^2 - P_o^2)}{2(P_i^3 - P_o^3)}$

The coefficient in the third term of the Golay equation, C_s, which describes diffusion in the stationary retentive layer, is sometimes neglected. Neglecting this term implies the adsorption-desorption mode of retention at the surface of the stationary phase and instantaneous (versus an actual slow) diffusion into the bulk of the material. In the earlier micro GC column work, Reston and Kolesar[11] attribute four orders of magnitude difference between their theoretical and experimental separation factors to this term. In addition, Golay indicates that this term can dominate in simple capillary columns; thus we have included this term in our design studies.

Separation experiments using a conventional capillary column (100 μm dia.) with a length of 1 m and nitrogen as a carrier gas have been performed to assess this analytical model. A comparison of retention between decane and dodecane in the 0.1-μm thick, SPB-5-coated column are shown in Fig. 4, as a function of pressure drop (or flow velocity). The model compares reasonably well within the uncertainty on the data, and it predicts the proper trends. Additional data is needed to understand and characterize the interaction between these many parameters defining the GC performance.

2.3. Design Evaluation

This analytical tool has been applied to evaluate the column performance for different geometries. Important parameters, such as number of theoretical plates, the HETP value, volumetric flow rate, and retention time, are calculated. If setting 30 sec. for the analysis time, results show that for the μChemLab™, a GC column with 40x250 microns cross section, 1 meter long, and a flow rate of 0.3 m/s will produce a reasonably good chromatographic performance (Fig. 5). This geometry will be the current baseline column design for the μChemLab™.

3. COMPUTATIONAL SIMULATION

The models presented in the previous section are derived based on the assumption that the flow in GC columns is a fully developed laminar flow with a parabolic velocity profile (a 2-D flow). This implies that the analyte transport in the transverse direction is by diffusion only. It neglects any convective transport in the cross-sectional plane, which may occur in a rectangular spiral column. For this geometry there may be a secondary flow at the corners and a recirculation flow generated from the curvature effect. To evaluate the accuracy of this 2-D flow assumption, we have simulated the transport dynamics with the MPSalsa code and compared its results with the analytical predictions.

3.1. MPSalsa Code

MPSalsa[12] is a computer program developed at Sandia to solve laminar, low Mach number, two- or three-dimensional

incompressible and variable density reacting fluid flows on massively parallel computers using a Petrov-Galerkin finite element formulation. It can analyze coupled fluid flow, heat transfer, multicomponent species transport, and finite-rate chemical reactions. The CHEMKIN library is employed to provide a rigorous treatment of multicomponent ideal gas kinetics and transport. MPSalsa has been designed to execute on different computer platforms from a workstation with single processor to massively parallel computers with thousands of processors. All of these MPSalsa simulations presented here are performed on a SUN Ultra-Sparc workstation and an Intel Paragon massively parallel computer.

3.2. Surface Interaction Model

Before performing any simulation, we developed and incorporated a time-dependent adsorption/desorption model in MPSalsa to model physico-chemical interactions between the analyte and the coated surface — i.e., the stationary phase. This leads to a modified boundary condition:

$$D_g \cdot \frac{\Delta c}{\Delta y} = -\left(k \cdot d \cdot \frac{\Delta c}{\Delta \tau}\right) \tag{5}$$

where y is normal to the surfaces. This expression implies that the total mass flux of analyte being adsorbed at the wall will be desorbed into those computational cells adjacent to the wall with a time delay controlled by the retention factor (k). At present this surface interaction model has neglected any penetration and diffusion of analyte into the stationary phase. However, in the future simulations the diffusion in the stationary phase will be included.

3.3. Results of Simulations

3.3.1. Defining the Problems of Interest

The baseline design of the GC column is a high aspect-ratio rectangular channel that is 40 μm wide and 250 μm deep and 1 m long. For modeling of two species transport (carrier gas and analyte), the required computational grid system is enormous — i. e., with a uniform grid size of about 4 μm — it will have about 15 million computational cells and 105 million unknowns to be solved. It becomes very computing intensive. Thus for this design study, only a section of the column will be analyzed to capture the curvature and corner effect instead of simulating the whole length of the GC column. A set of simulations have been performed to study the analyte transport,[13] and results of two simulations will be presented here.

3.2.2. A 180-Degree Curved 40-μm Column

This simulation is used to investigate the analyte transport in a 180-degree curved column. Because of the limitation in the computer resources, the simulated 40-μm wide column is only 40 μm deep instead of 250 μm. However, this setup should be sufficient to study the corner effect of the column. The radius of curvature of this column (R) is 270 μm, which is approximately equal to the smallest radii of curvature in the spiral configuration. The length of the simulated column is 1 mm, and the pressure drop across the column segment is 126 Pa. This pressure drop will produce a flow velocity similar to the velocity in the baseline design. Also in this simulation we have investigated the effect of asymmetric coating of stationary phase on the analyte transport. This setup has the coating of stationary phase only applied on the side walls but not to the top and bottom walls. Hence surface interactions will be confined to the side walls.

The MPSalsa simulation of analyte transport in this 3-D column is interesting. The analyte concentration profile is mostly flat in the vertical direction (Fig. 6). Hence under these conditions (a 40-mm wide column with a flow velocity of about 0.3 m/s), it behaves like a 2-D flow with minimal curvature effect. Dean number, which is the ratio of centrifugal force to viscous force, is a good way to judge the curvature effect. $De = (\rho u d)/\mu \cdot \sqrt{d/(2R)}$. Therefore, it is proportional to the square root of the ratio of the column width to the radius of curvature. The higher the Dean number, the more influence the curvature effect will be. In this problem the Dean number is very small at about 0.2.

Regarding the effect of asymmetric coating, there is a slight difference of concentration profile at the top wall than at the side wall. Since the top and bottom walls are not coated while the side walls are coated, the migration speed of analyte near the side walls is slower than the speed near the top and bottom walls. In this case the difference is relatively small. However, in other cases the difference can be large and may eventually lead to a larger band spreading. Therefore, a symmetric uniform coating of all four walls with stationary phase is recommended; though, it may be difficult to apply for this baseline GC column.

This simulation also demonstrates the ability of the code to predict separation of analytes. Simultaneous transport of two analytes (1 percent Dimethyl methyl phosphonate or DMMP and 1 percent Benzene) have been modeled with air as the carrier gas. DMMP and benzene have different molecular weight, 124.08 versus 78.11, respectively, and different binary diffusion coefficient, 0.146×10^{-4} m^2/s versus 0.096×10^{-4} m^2/s. Simulation results show these two analytes migrate downstream at different speeds. Each interacts differently with stationary phase coated on the wall; retention factors of 1 and 5 are used.

3.3.2. A 180-Degree Curved 100-μm Column

The second simulation is a sensitivity study. For some cases where the condition has changed, the curvature effect can be significant. In this study the column dimension and the flow velocity have been increased. The new column is 100 μm wide, and the new flow velocity at the entrance of the 1 mm column is 5 m/s. The new Dean number is 13, which is much larger than the previous case. Similarly the Reynolds number and Peclet number will be larger as well.

With this new condition, MPSalsa predicts a different concentration profile. In this case the profile is very discrete, elongated, and twisted (Fig. 7). This unique feature is generated from the fluid being convected downstream around a curved channel. Substantial shear in the fluid occurs that later develops into local vortices. The analyte migrating at the outer wall is lagging behind the analyte migrating at the inner wall. This leads to a broader band spreading. Hence the curvature effect is more significant when flow rate increases or column size increases. This contribution to band spreading is not modeled in the analytical tool for the GC column design.

4. CONCLUSIONS

For the μChemLab™ project, we have developed valuable tools (both analytical models and computer simulations) to analyze complex transport phenomena in the GC columns. These tools can guide the column design and reduce the number of iterations in the device development. The analytical models consist of a flow module and a separation module. The flow module models compressibility and slip flow effects, which are significant in gas flow in a long and narrow column. The separation module predicts column performance based on the modified Golay equation. Both models have been assessed well against experimental data.

Computational simulations have been performed to investigate the geometric effect on analyte transport, which the analytical models fail to capture. This study is to investigate the potential secondary flow near the corner and the recirculation flow generated from the curvature of the column. Simulation results show that it can capture the complex flow and transport dynamics better than the analytical models. Simulations also reveal that amongst the GC column geometries being studied, the desired geometry (40-micron wide channel) and flow condition (velocity of 0.3 m/s) will give a reasonably good performance of chromatography. This supports the finding from the analytical models. However, if the condition changes, a wider column and/or a larger flow velocity, complex flow structure can be generated from the curvature of the column leading to a substantial band spreading that will degrade the chromatographic performance.

ACKNOWLEDGEMENT

This work was funded by the Sandia National Laboratories, Laboratory Directed Research and Development (LDRD) program. Sandia is a multiprogram laboratory operated by Sandia Corporation, a Lockheed Martin Company, for the United States Department of Energy under contract number DE-AC04-94AL85000.

REFERENCES

1. D. W. Arnold, C. G. Bailey, M. G. Garguilo, C. M. Matzke, J. R. Wendt, W. C. Sweatt, S. H. Kravitz, M. E. Warren, and D. J. Rakestraw, "Microseparations and Microfluidic Studies," *Proceedings of the 3rd International Symposium on Micro Total Analysis System*, Banff, Alberta, Canada, pp. 435-436, 1998.
2. G. C. Frye-Mason, R. J. Kottenstette, E. J. Heller, C. M. Matzke, S. A. Casalnuovo, P. R. Lewis, R. P. Manginell, W. K. Schubert, and V. M. Hietala,, "Integrated Chemical Analysis Systems for Gas Phase CW Agent Detection," *Proceedings of the 3rd International Symposium on Micro Total Analysis System*, Banff, Alberta, Canada, pp. 477-478, 1998.
3. D. W. Grant, *Capillary Gas Chromatography*, John Wiley & Sons, Chichester, United Kingdom, 1996.

4. B. L. Karger, L. R. Snyder, and C. Horvath, *An Introduction to Separation Science*, John Wiley & Sons, New York, 1973.
5. C. M. Matzke, R. J. Kottenstette, S. A. Casalnuovo, G. C. Frye-Mason, M. L. Hudson, D. Y. Sasaki, R. P. Manginell, and C. C. Wong, "Microfabricated Silicon Gas Chromatographic Micro-Channels: Fabrication and Performance," *Proceedings of the SPIE Conference on Micromachining and Microfabrication Process Technology IV*, Santa Clara, CA, Vol. 3511, pp. 262-268, 1998.
6. F. M. White, *Viscous Fluid Flow*, McGraw Hill, New York, pp. 200-215, 1974.
7. G. A. Bird, *Molecular Gas Dynamics and Direct Simulation of Gas Flows*, Clarendon Press, Oxford, United Kingdom, 1994.
8. M. J. Golay, "Theory of Chromatography in Open and Coated Tubular Columns with Round and Rectangular Cross-Sections," *Gas Chromatography*, D. H. Desty, ed., Academic Press, New York, pp. 36-55, 1958.
9. L. S. Ettre and J. V. Hinshaw, *Basic Relationships of Gas Chromatography*, Advanstar, Cleveland, Ohio, 1993.
10. M. L. Hudson, R. J. Kottenstette, C. M. Matzke, G. C. Frye-Mason, K. A. Shollenberger, D. R. Adkins, and C. C. Wong, "Design, Testing, and Simulation of Microscale Gas Chromatography Columns," *ASME DSC-Vol. 66, MEMS 1998*, ASME 1998 International Mechanical Engineering Congress and Exposition, Anaheim, CA, pp. 207-214, 1998.
11. R. R. Reston and E. S. Kolesar, "Silicon-Micromachined Gas Chromatography System Used to Separate and Detect Ammonia and Nitrogen Dioxide — Part II: Evaluation, Analysis, and Theoretical Modeling of the Gas Chromatography System," *Journal of Microelectromechanical Systems*, Vol. 3, No. 4, pp. 147-154, Dec. 1994.
12. J.N. Shadid, A. Salinger, H. K. Moffat, S. A. Hutchinson, G. L. Henningan, and K. D. Devine, *MPSalsa, a Finite Element Computer Program for Reacting Flow Problems, Part 1 - Theoretical Development, SAND95-2752, Part 2 - User Guide, SAND96-2331*, Sandia National Laboratories, Albuquerque, NM, 1996.
13. C. C. Wong, "Simulations of Species Transport in GC Columns," *Sandia Internal Memorandum*, July 9, 1998.

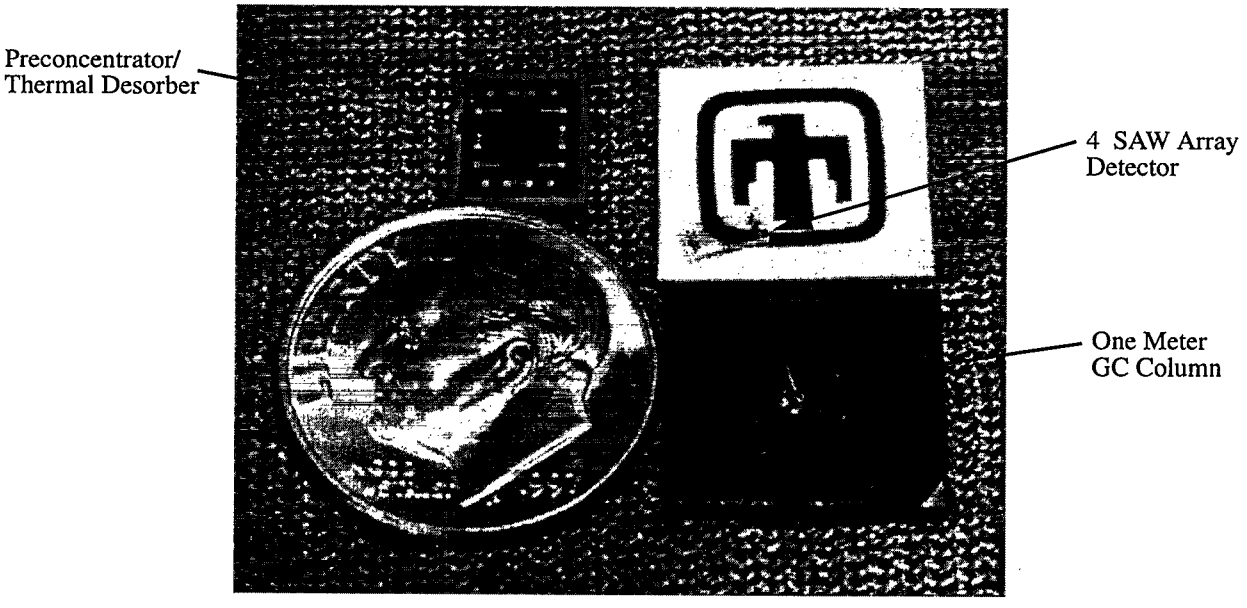

Figure 1. Picture of Different Components in μChemLab™; proceeding clockwise: a U.S. dime (18 mm diameter), Preconcentrator, SAW array detector, and GC Column).

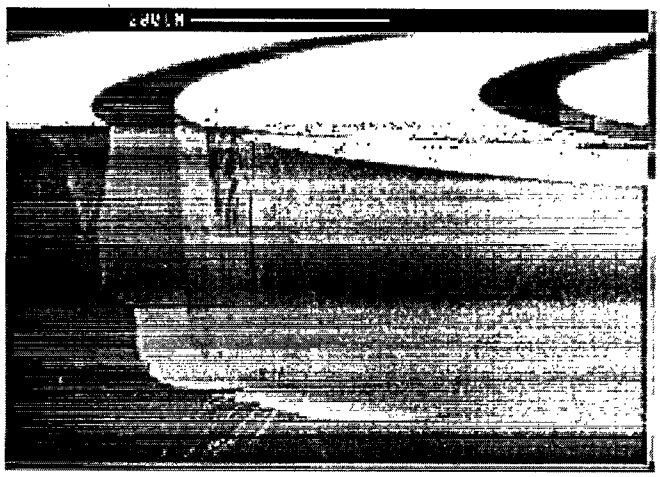

Figure 2. Cross section SEM of a GC column fabricated in silicon by Bosch reactive ion etching process.

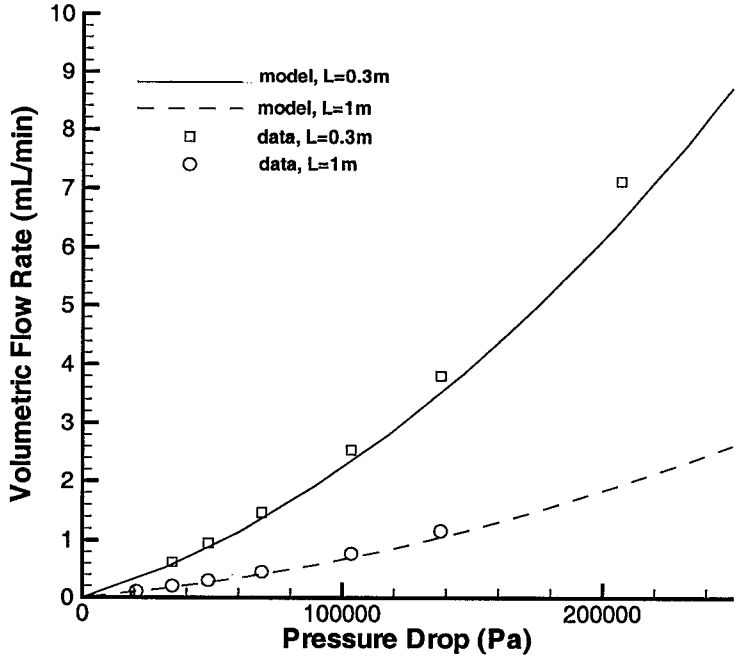

Figure 3. Comparison of the volumetric flow rate in spiral rectangular columns as a function of pressure drop between predictions and experimental data (air, 40μm x 250 μm column).

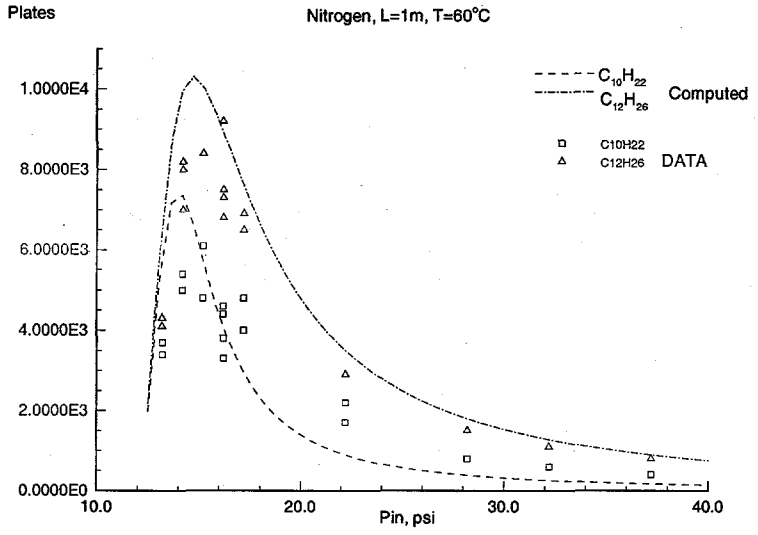

Figure 4. Comparison of GC performance between predictions and data: number of theoretical plates versus inlet pressure (capillary tube of 100 μm diameter and 1 m long, nitrogen, 60-degree C).

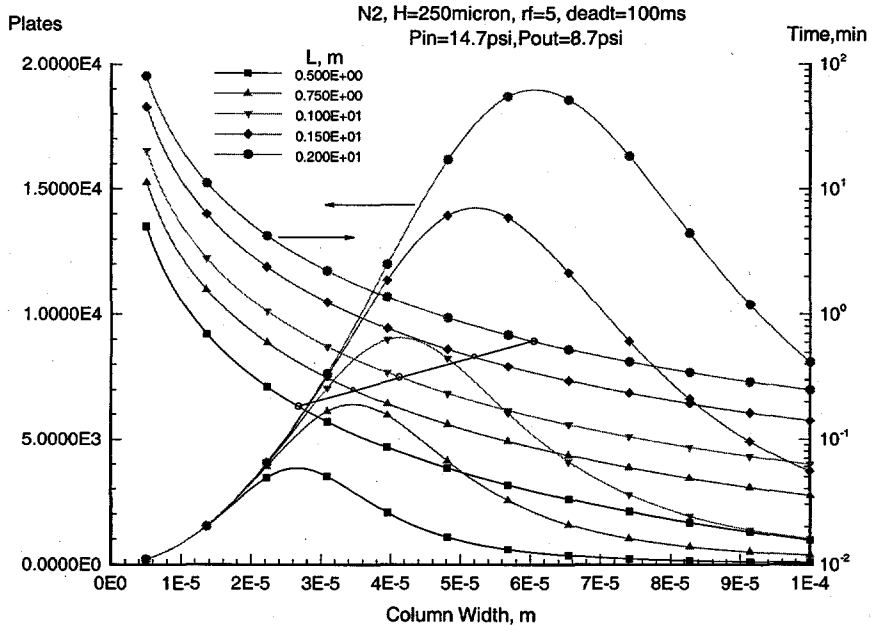

Figure 5. Design study for the spiral rectangular GC columns: plate number and run time versus column width; column depth=250 μm, pressure drop=40 kPa (6 psi), retention factor=5, dead time=100ms.

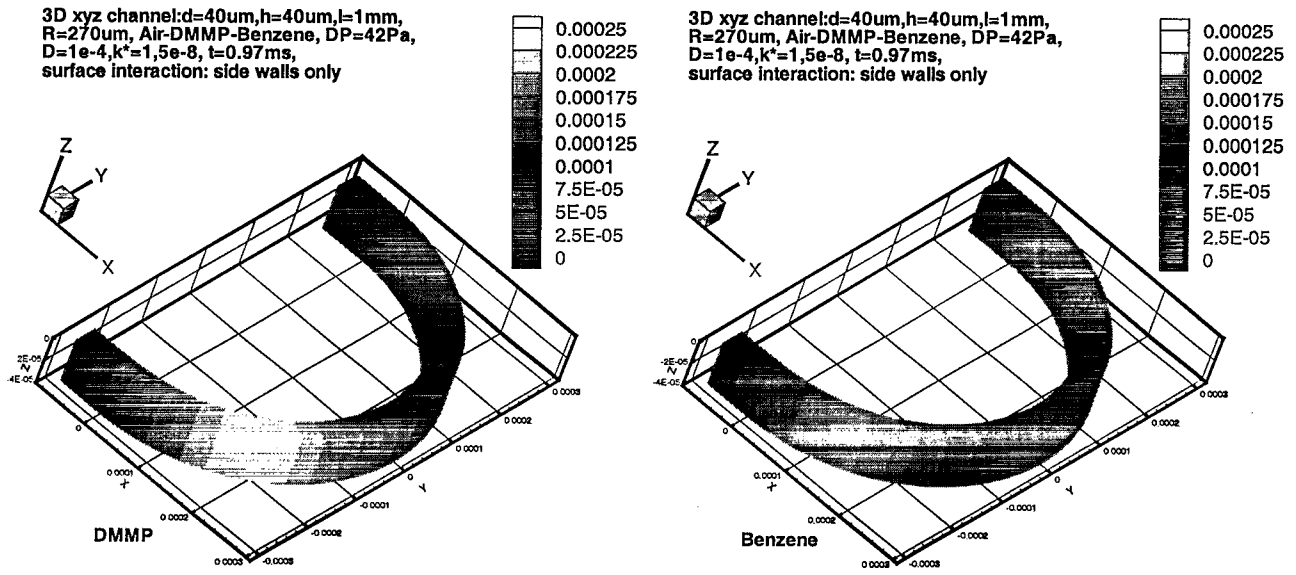

Figure 6. Concentration profile for DMMP and benzene to illustrate the simulated separation of analytes in the GC column.

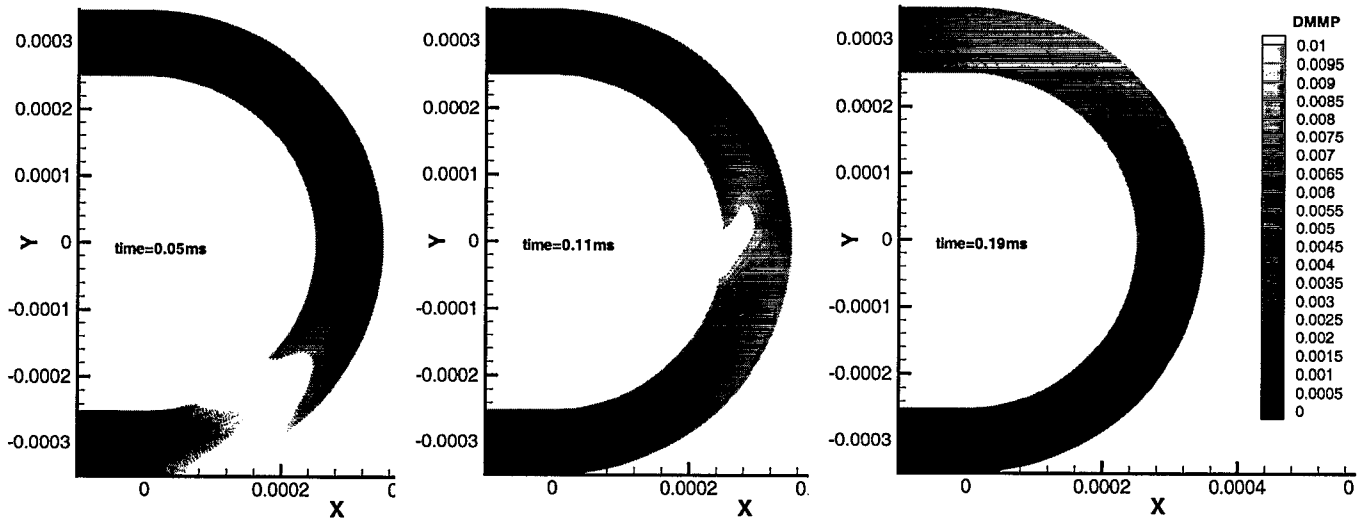

Figure 7. Concentration profile of DMMP migrating along a 100-μm wide GC column showing the complexity of transport dynamics.